remote sensing

MDPI

Article

Assessment of Radiometric Calibration Consistency of Thermal Emissive Bands Between Terra and Aqua Moderate-Resolution Imaging Spectroradiometers

Tiejun Chang [1,*], Xiaoxiong Xiong [2], Carlos Perez Diaz [1], Aisheng Wu [1] and Hanzhi Lin [1]

[1] Science Systems and Applications, Inc., Lanham, MD 20706, USA
[2] Sciences and Exploration Directorate, National Aeronautics and Space Administration Goddard Space Flight Center, Greenbelt, MD 20771, USA
* Correspondence: tiejun.chang@ssaihq.com

Abstract: Moderate-Resolution Imaging Spectroradiometer (MODIS) sensors onboard the Terra and Aqua spacecraft have been in orbit for over 24 and 22 years, respectively, providing continuous observations of the Earth's surface. Among the instrument's 36 bands, 16 of them are thermal emissive bands (TEBs) with wavelengths that range from 3.75 to 14.24 μm. Routine post-launch calibrations are performed using the sensor's onboard blackbody and space view port, the moon, and vicarious targets that include the ocean, Dome Concordia (Dome C) in Antarctica, and quasi-deep convective clouds (DCC). The calibration consistency between the satellite measurements from the two instruments is essential in generating a multi-year data record for the long-term monitoring of the Earth's Level 1B (L1B) data. This paper presents the Terra and Aqua MODIS TEB comparison for the upcoming Collection 7 (C7) L1B products using measurements over Dome C and the ocean, as well as the double difference via simultaneous nadir overpasses with the Infrared Atmospheric Sounding Interferometer (IASI) sensor. The mission-long trending of the Terra and Aqua MODIS TEB is presented, and their cross-comparison is also presented and discussed. Results show that the calibration of the two MODIS sensors and their respective Earth measurements are generally consistent and within their design specifications. Due to the electronic crosstalk contamination, the PV LWIR bands show slightly larger drifts for both MODIS instruments across different Earth measurements. These drifts also have an impact on the Terra-to-Aqua calibration consistency. This thorough assessment serves as a robust record containing a summary of the MODIS calibration performance and the consistency between the two MODIS sensors over Earth view retrievals.

Keywords: Moderate-Resolution Imaging Spectroradiometer; thermal emissive bands; Collection 6.1; Collection 7; Level 1B; intercomparison; Terra; Aqua; calibration; radiometric

Academic Editor: Jian Xu

Received: 22 November 2024
Revised: 26 December 2024
Accepted: 30 December 2024
Published: 7 January 2025

Citation: Chang, T.; Xiong, X.; Diaz, C.P.; Wu, A.; Lin, H. Assessment of Radiometric Calibration Consistency of Thermal Emissive Bands Between Terra and Aqua Moderate-Resolution Imaging Spectroradiometers. *Remote Sens.* **2025**, *17*, 182. https://doi.org/10.3390/rs17020182

1. Introduction

The Moderate Resolution Imaging Spectroradiometer (MODIS) is one of the key instruments on National Aeronautics and Space Administration (NASA) Earth Observing System. One MODIS is on the Terra satellite platform, while the other is onboard Aqua. With over two decades of data records, these two instruments have been providing continuous observations of the Earth's surface and play a vital role in the development of validated, global, interactive Earth system models that are able to predict global change accurately enough to assist policy makers in making sound decisions concerning the protection of our environment [1–8]. There are 36 spectral bands on the MODIS sensors covering visible,

near-infrared, shortwave, midwave, and longwave infrared spectra. Among the 36 MODIS bands, 16 of them are thermal emissive bands (TEBs) whose wavelengths range from 3.75 to 14.24 μm (Table 1). The MODIS TEBs are located on two focal plane assemblies (FPA). The photovoltaic (PV) midwave infrared (MWIR) bands, 20–25, are on the shortwave/midwave infrared (SWIR)/MWIR FPA, while the longwave infrared (LWIR) bands, 27–36, are on the LWIR FPA. These FPA are controlled at stable low temperatures (~83 K).

Table 1. MODIS TEB characteristics and primary applications. (CW: center wavelength; BW: bandwidth, T_{TYP}: typical temperature, NEdT: noise equivalent temperature difference).

Band Group	TEB Band	CW (μm)	BW (μm)	T_{TYP} (K)	NEdT (K)	Primary Use
PV MWIR	20	3.75	0.18	300	0.05	Surface/cloud temperature
	21	3.96	0.06	335	0.20	
	22	3.96	0.06	300	0.07	
	23	4.05	0.06	300	0.07	
	24	4.47	0.07	250	0.25	Atmospheric temperature
	25	4.52	0.07	275	0.25	
PV LWIR	27	6.72	0.36	240	0.25	Water vapor
	28	7.33	0.30	250	0.25	
	29	8.55	0.30	300	0.05	Cloud properties
	30	9.73	0.30	250	0.25	Ozone
PC LWIR	31	11.03	0.50	300	0.05	Surface/cloud temperature
	32	12.02	0.50	300	0.05	
	33	13.34	0.30	260	0.25	Cloud top altitude
	34	13.64	0.30	250	0.25	
	35	13.94	0.30	240	0.25	
	36	14.24	0.30	220	0.35	

The quality and accuracy of the calibrated imagery produced by the two instruments throughout their operating lifetime require regular monitoring of their radiometric performance, which is achieved by the suite of onboard calibrators for both the reflective and thermal spectral regions. Routine post-launch calibrations for the MODIS TEBs are performed using the onboard blackbody (BB), the moon, and vicarious targets that include the ocean, Dome Concordia (Dome C) in Antarctica, and quasi-deep convective clouds (DCC).

The intercomparison between the Terra and Aqua MODIS measurements is extremely important when assessing their calibration accuracy, as well as their consistency with regard to the higher-level science products derived from them. One such example is the consistency between the Terra and Aqua MODIS cloud products used for the MODIS calibration uncertainty assessment. The calibration consistency between the satellite measurements from the two instruments is essential in generating a reliable multi-year data record for the long-term monitoring of the Earth's Level 1B (L1B) data products. Likewise, this consistency is also critical for higher-level science products. This manuscript focuses on the comparison between the Terra and Aqua MODIS TEB L1B products for the upcoming Collection 7 (C7). This paper can be used as a reference for any C7-related L1B product assessments and to evaluate the consistency of any science products associated with them.

Section 2 presents an overview of the MODIS TEB calibration, with a focus on the C7 calibration algorithm and the most impactful improvements made over the previous Collection 6.1 (C6.1) version. Section 3 describes the inter-comparison methodology, while Section 4 illustrates the Terra and Aqua MODIS TEB comparison results using measurements over Dome C and the ocean, as well as from simultaneous nadir overpasses with the

Infrared Atmospheric Sounding Interferometer (IASI) sensor as references. The results are discussed and summarized in Sections 5 and 6, correspondingly.

2. MODIS Calibration Overview

2.1. MODIS TEB Calibration Overview

The MODIS TEB includes 16 bands from the total of 36 bands. MWIR bands 20–25 cover wavelengths 3.8 through 4.5 μm, while the LWIR bands from 27 to 36 spectra range from 6.8 to 14.2 μm. The nominal MODIS TEB calibration is a two-point calibration performed via the response to the MODIS onboard BB and space view (SV), which serve as the primary calibration sources. Each detector views the BB and SV every scan to calibrate the on-orbit gain. The BB temperature is set to a fixed value during nominal operation (currently at 285 K for both MODIS instruments while it was at 290 K for Terra MODIS before April 2020). The TEB calibration is based on a quadratic algorithm which converts the digital response of the sensor to calibration radiance (L_{CAL}) [7–9]. For each TEB detector and scan-mirror (SM) side, the calibration uses a quadratic calibration algorithm, $L_{CAL} = a_0 + b_1 dn_{BB} + a_2 dn_{BB}^2$, where a_0 and a_2 are the offset and non-linear coefficients, dn_{BB} is the background-subtracted detector digital response when viewing the BB, and b_1 is the linear coefficient. The non-linear and offset terms are obtained from an offline look-up table (LUT) that is updated periodically, and the BB warm-up and cooldown (WUCD) operation is used to characterize and update the instrument's non-linear response coefficients in orbit. The BB WUCD operation is performed quarterly, and its temperature is programmed to change from the instrument's ambient temperature (about 270 K) to 315 K. For the nominal operation and WUCD calibration from both sensors, the calibration radiance (L_{CAL}) from the BB view is defined as follows:

$$L_{CAL} = RVS_{BB}\varepsilon_{BB}L_{BB} + (RVS_{SV} - RVS_{BB})L_{SM} + RVS_{BB}(1 - \varepsilon_{BB})\varepsilon_{cav}L_{cav} \quad (1)$$

where ε is the emissivity of the BB or cavity (cav) where all the MODIS on-board calibrators are. It is held at a constant temperature. And for the sake of the TEB calibration, any radiation reflected from the BB into MODIS (mainly from the scan cavity walls) is considered to be part of the cavity radiance, L is the radiance from the BB, SM, or cavity, and RVS is the response-versus-scan-angle at the SV or BB view. b_1 is the scan-by-scan linear coefficient, and its calibration during nominal operation can be performed using the emissivity, RVS, and non-linear coefficients from LUT as follows:

$$b_1 = \left[L_{CAL} - a_0 - a_2 dn_{BB}^2\right] / dn_{BB} \quad (2)$$

Lastly, the following equation is used for the Earth view (EV) radiance retrievals:

$$L_{EV} = \frac{1}{RVS_{EV}}\left[a_0 + b_1 dn_{EV} + a_2 dn_{EV}^2 - \left(RVS_{SV} - RVS_{EV}\right)L_{SM}\right] \quad (3)$$

where RVS_{EV} is the EV RVS as a function of mirror incident angle. The TEB RVS comes from pre-launch tests for Aqua MODIS and from post-launch using pitch maneuvers for Terra MODIS [10–13].

2.2. Terra and Aqua MODIS TEB C7 Calibration Algorithm

The calibration algorithm described in Section 2.1 applies to both the Terra and Aqua MODIS TEB and was used to build a consistent foundation between their respective L1B products. However, the MODIS TEB algorithm is implemented differently between Terra and Aqua when in operation. Part of the reason is in how the calibration coefficients derived from the prelaunch test results are applied to the on-orbit calibration. The previous litera-

ture presents detailed descriptions of these differences for C6.1 [7–9,14]. In C7, the MODIS Characterization Support Team (MCST) made substantial efforts to improve the on-orbit calibration accuracy and consistency between the MODIS sensors (see Table 2 for the Terra and Aqua MODIS C7 calibration algorithm for all TEB) [15–17]. Improvements considered to be major include the use of L1B measurements over cold Earth targets (qDCC and Dome C) to correct drifts and mirror side differences and to mitigate additional electronic crosstalk contaminations for image striping removal and radiometric bias corrections.

Table 2. Calibration algorithm for all Terra and Aqua MODIS TEB in C7. OO: on-orbit; PL: prelaunch; MS: mirror side; coeffs: coefficients; corr: correction; N/A: not applicable.

Band	Aqua			Terra		
	Calibration Coeffs.		Crosstalk Coeffs.	Calibration Coeffs.		Crosstalk Coeffs.
	a_0	a_2		a_0	a_2	
20	PL + MS corr.	OO	Electronic crosstalk correction for select detectors	OO + drift corr. + MS corr.	OO	N/A
21	Zero	Zero		Zero	Zero	N/A
22	PL + MS corr.	OO		OO Before 03/2022: MS1 = 0 MS2 = MS2-MS1 After 03/2022: MS1 = MS1-MS2 MS2 = 0	OO	Electronic crosstalk correction for select detectors
23						
24						
25						
27	PL + MS corr. + cold scene corr.		Electronic crosstalk correction for all detectors + EV adjustment			Electronic crosstalk correction for all detectors
28						
29				OO + drift corr. + MS corr		
30		Fixed to 2012		Fixed from 2003 to 2010 + MS corr., then OO	Fixed from 2003 to 2010, then OO scaled using factor	
31	Zero	OO	N/A	Zero	OO	N/A
32				Zero		N/A
33		PL adjusted OO		Early mission: MS corr. Starting 2003: Zero		Optical crosstalk correction for all detectors
34						
35						
36						

Signal contamination in the form of electronic crosstalk has been observed in many of the TEBs since pre-launch. This became particularly evident for Terra MODIS bands 27–30 after the instrument underwent a safe mode event in February 2016. These electronic crosstalk effects impact the L1B and higher-level products, causing image artifacts such as striping and radiometric biases. Hence, electronic crosstalk corrections were applied shortly after and delivered in the form of C6.1. MCST is also aware that some detectors in the Terra MODIS midwave infrared (MWIR) bands show signs of electronic crosstalk contamination. In Terra MODIS C7, electronic crosstalk corrections are applied to these detectors as well. In the case of Aqua MODIS, while it can be observed in many of the TEBs, the electronic crosstalk contamination is significantly smaller when compared to the same bands for Terra MODIS. However, the March 2022, Aqua safe mode induced a significant increase in the electronic crosstalk between its MODIS PV LWIR bands. MCST thus decided to apply electronic crosstalk corrections to these bands in forward production starting at the safe mode timeline for Aqua MODIS C6.1. In Aqua MODIS C7, these corrections are applied from mission beginning in addition to corrections to some detectors in the MWIR bands. Table 3 lists the relative changes from C6.1 to C7.

Table 3. Major improvements made to the Terra and Aqua MODIS TEB in C7 relative to C6.1.

Terra	Aqua
MWIR bands' electronic crosstalk correction for select detectors	MWIR bands electronic crosstalk correction for select detectors
Early mission MS difference correction for photoconductive bands	PV LWIR bands' electronic crosstalk correction and calibration algorithm improvement
Bands 20 and 29 drift and MS correction to improve stability over colder scenes	Adjustment in band 30 non-linear coefficient to improve trending stability
Band 30 calibration algorithm adjustments to improve calibration stability	Mission-long MS difference correction and use of on-orbit data to improve long-term stability of the PV bands

Generally, crosstalk occurs between bands and detectors that are located on the same focal plane assembly. The source of the contaminating signals can be identified using lunar and EV data. The contaminating signal has been assumed to be linearly proportional to the measured signal from the identified sending bands. Since electronic crosstalk affects the digital signal in each data sector, it will have an impact on the background signal and the signal from any measured EV or OBC scene. However, since the background contamination is at a nearly constant level, this contamination can be subtracted off with the rest of the background signal. To oversimplify, the crosstalk coefficients, ci and j, are in the form of a matrix which contains linear coefficient values that connect a detector's receiving contamination i, to each of the detectors that send contamination j. Once the correction coefficients are obtained, the correction is applied to the background-subtracted digital counts, dn, for each data sector to derive the calibration coefficients and EV scene radiance. Thus, the corrected signal at the pixel level can be written as follows: $dn_i(S,F) = dn_i^*(S,F) - \sum_j c_{i,j} dn_j^*\left(S,\ F + \Delta F_j\right)$. Here, S and F represent the scan and frame numbers, respectively; ΔFj is the relative frame offset of detector j with respect to detector i; and the * represents the digital count before the correction is applied. A detailed description of the correction and its impact on the L1B data is described by Wilson et al. and in the 2018 MODIS TEB electronic crosstalk workshop [18,19]. In Section 3, we will show the increase in electronic crosstalk for the MODIS PV LWIR bands after both safe mode anomalies as well as the impacts these had on the L1B products via image assessment.

3. TEB Intercomparison Methodology

3.1. TEB Calibration and Intercomparison Assessment

Inter-comparisons between the Terra and Aqua TEBs have been conducted using early versions of the MODIS L1B products. Additionally, NASA ER-2 aircraft-based measurements have been used to assess the radiometric performance of Terra and Aqua MODIS Collection 5 radiances for LWIR bands 31–36 [20]. This paper focuses on the mission-long Terra and Aqua intercomparison for the latest version of the NASA MODIS L1B products (i.e., C7) for all the MODIS TEBs. The comparison is performed over different Earth scene types and by comparing MODIS to the IASI instrument. This assessment will be an extremely valuable addition to the MODIS literature records and will help evaluate any higher-level products associated with them in the future. This aircraft was used as a dedicated remote sensing platform that was coordinated with satellite observations during their respective overpass times and orbits. Near-surface automated observations at Lake Tahoe, CA/NV, USA, and Salton Sea, CA, USA, have also been used to validate thermal infrared radiometers, including Advanced Spaceborne Thermal Emission and Reflection Radiometer (ASTER), MODIS, and the Visible Infrared Imaging Radiometer Suite (VIIRS) [21]. Moreover, temperature measurements near the surface at extremely cold conditions obtained over Dome C, Antarctica, were used to examine the Terra and

Aqua MODIS stability and inter-calibration consistency [22–24]. Similar approaches to those used for Dome C have been applied to earth scene at higher temperatures, i.e., examining with sea surface temperature (SST) measurements from floating buoys [25,26]. Observations from the Atmospheric Infrared Sounder (AIRS) and MODIS (both on the same Aqua platform) have provided highly accurate MODIS calibration assessments using well-calibrated hyperspectral data from AIRS. This can be achieved after the high spectral resolution AIRS data are reduced to the MODIS spectral resolution, and the high spatial resolution MODIS data are reduced to the AIRS spatial coverage [27].

Observations obtained from the simultaneous nadir overpass (SNO) between MODIS and IASI on the Metop-A satellite have been used to evaluate the MODIS radiometric accuracy and the relative differences between Terra and Aqua with IASI as a transfer radiometer [28,29]. These comparisons largely confirm that the atmospheric window bands 31 (11 μm) and 32 (12 μm) of MODIS perform well within the 0.5% radiometric specification throughout the mission. The LWIR bands 34–36 are found to be performing outside of their 1% accuracy specification, with larger biases for Terra MODIS. While large biases, striping, and drifting are observed for Terra MODIS bands 27 to 30 in the Collection 6 L1B product due to electronic crosstalk, the performance of these bands are significantly improved in the Collection 6.1 calibration algorithm in which an electronic crosstalk correction was developed and applied, as shown in the comparison results [18].

The IASI instruments onboard the series MetOp satellites provide hyperspectral measurements of the atmosphere in the IR spectrum covering wavelengths from 3.4 to 15.5 μm (all 16 MODIS TEBs are thus spectrally comparable to IASI). The MetOp satellites are in sun-synchronous polar orbits, similar to the Terra and Aqua satellites, and have SNO with the Terra and Aqua satellites over high-latitude areas. Therefore, the SNO makes it possible to compare the MODIS L1B nadir measurements with the IASI Level 1C (L1C) data. Afterwards, the double difference against IASI can be used to compare the Terra and Aqua MODIS TEBs.

MetOp-A, Europe's first polar-orbiting satellite for operational meteorology, was launched on 19 October 2006 and started deorbiting in 2021, and MetOp-C was launched in November 2018 and is currently in operation. Using an appropriate arrangement of data from both IASI sensors, MODIS and IASI can be intercompared from 2007 to the present time. All orbit parameters for the satellites were obtained from two-line element sets. The SNO time between Terra (or Aqua) and MetOp can be determined (or predicted) within 30 s for each SNO data collection. The corresponding IASI L1C and MODIS L1B and geolocation granules during the SNO period were selected and processed. During the SNO pixel selection process, the IASI pixels were chosen from two instantaneous field of view (IFOV) pairs at nadir (approximately 3.3° off nadir), while the MODIS pixels were in a range of ±10° off nadir to collect enough sample data. The MODIS TEB pixel size (1 km at nadir) is much smaller than IASI's (12 km at nadir). Hence, the MODIS pixels were averaged to match the IASI footprint.

Dome C is located on the Antarctic Plateau (75.1° S, 123.4° E). The site is within a large snow flat surface on the Antarctic Ice Sheet with a high elevation of about 3200 m. The atmospheric conditions are exceptionally cold and dry with very little or no precipitation throughout the year. These conditions make Dome C an excellent site for use as a ground pseudo-invariant calibration target for remote sensing satellites. A further advantage is there is an Automated Weather Station (AWS) operating at the site since 1995 (operated jointly by the French Institut Polaire Francais Paul Emile Victor (IPEV) and the University of Wisconsin). The AWS provides air temperature, barometric pressure, and wind speed/direction measured at 3.0 m above the surface at 10 min intervals using standard meteorological sensors [30].

The AWS surface temperature data of Dome C is used to track calibration stability and consistency between the Terra and Aqua MODIS TEBs. For each MODIS overpass over Dome C, the coincident AWS surface temperature is extracted for comparison. Although the AWS temperatures are not directly comparable with the MODIS brightness temperature (BT) obtained at top of atmosphere, with an assumption of good correlation between the two, they do provide a useful proxy to track drifts and relative biases for the MODIS TEB on average over the long term. This approach has been found to work well for atmospheric window bands such as MODIS bands 31 and 32 [23–25]. The difference between the MODIS BT and AWS temperature is calculated for each TEB. The MODIS BT values are obtained by averaging over 20 × 20 pixels centered around Dome C. The matched BT and AWS pairs are collected each overpass and averaged over a period of 30 days to remove daily fluctuations. Overpasses with cloud contamination are removed based on the MOD06 (Terra) or MYD06 (Aqua) cloud product information. A relative temperature difference between the two MODIS is calculated using the double difference method. Since coincident MODIS and AWS data are used, the magnitude of the seasonal oscillation can be significantly reduced in the trends of the relative bias between Terra and Aqua MODIS.

As part of the vicarious calibration practices, natural or artificial sites on the Earth's surface are often used to calibrate sensors post-launch. These locations are frequently used as an alternative to the common on-orbit calibration methods used to monitor sensor performance as well as the inter-sensor comparison approaches. While Dome C takes care of the on-orbit calibration consistency assessment between the two MODIS sensors over colder scenes, an ocean (natural) site offers the possibility of evaluating such performance over the more typical warmer temperatures. In this study, coordinates over a NOAA-owned ocean site in the Pacific Ocean near Sand Island, HI, USA, are used to define the ocean location used to intercompare the Terra and Aqua MODIS TEBs. This site has been used previously to evaluate the calibration accuracy of the MODIS instruments [26].

The MODIS Level 1A (L1A), geolocation, and cloud mask data were retrieved for the granules overlooking the ocean site. Only nighttime granules were used for the analysis. The MODIS L1A EV digital counts were converted to BT using the C7 calibration look-up tables, each band's spectral response function, and Planck's law. The MODIS pixels (20 km by 20 km area) over the precise ocean location were extracted and cloud-covered pixels were filtered out (only "probably clear" or "confident clear" flag designations were considered) using the MODIS cloud mask data prior to any examination. The remaining valid pixels were normalized to their corresponding band 31 BT. Afterward, the average BT was calculated for each available overpass. Finally, in order to compare the TEBs between the two MODIS sensors, the average monthly results were used, since the instruments do not share the same overpass time over the scene and only a handful of nighttime granules are available per month. Since all nighttime granules are used, any view angle effects caused by non-nadir overpasses are corrected using the methodology developed by Chang and Xiong [31]. It should also be noted that prior to converting the radiances to BT, the Terra radiances were adjusted using the spectral correction factor discussed in Section 3.2. This factor is used to reduce spectral differences between the Terra and Aqua MODIS TEBs.

3.2. Correction for Spectral Differences Between Terra and Aqua MODIS TEBs

There are known spectral differences between some of the Terra and Aqua MODIS bands [32]. Normally, a spectral correction is used to minimize the impact these differences have on any Terra–Aqua comparison. In this study, a typical radiance spectrum was simulated (Figure 1) using MODerate resolution atmospheric TRANsmission (MODTRAN) 5.0 to derive this correction and use it to account for mismatches in the relative spectral response (RSR) caused by spectral differences between the Terra and Aqua MODIS TEBs

as well as variations in the predominant columnar atmospheric water vapor over ocean scenes [33]. The MODIS Atmospheric Profile products—which contain pertaining inputs for MODTRAN simulations such as atmospheric layer elevation, pressure, water vapor mixing ratio, and temperature—were used to provide the columnar atmospheric water vapor information [34]. These parameters are produced daily at a 5x5 1 km pixel resolution when at least nine FOV are cloud-free. Hence, any heavily cloud-covered granules were excluded from the simulation.

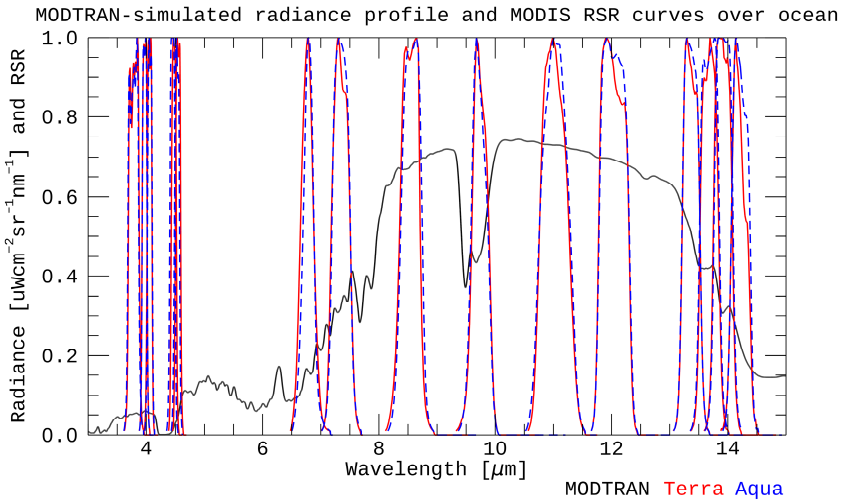

Figure 1. MODTRAN profile over an ocean scene simulated using MODIS Atmospheric Profile product as input. MODIS RSR are superimposed over the MODTRAN simulation.

MODTRAN can provide the spectral signature of a typical tropical ocean scene at a fine spectral resolution of 1 nm. This high spectral resolution is fundamental when characterizing the impacts of various water vapor absorption features on the retrieved top-of-atmosphere radiance. Using this high-resolution spectral profile, a Spectral Band Adjustment Factor (SBAF) can be calculated as follows:

$$SBAF = \frac{\sum_{i=1}^{n} \frac{\frac{\int_{\lambda_1}^{\lambda_2} L_{MODTRAN} RSR_{Terra} d\lambda}{\int_{\lambda_1}^{\lambda_2} RSR_{Terra} d\lambda}}{\frac{\int_{\lambda_1}^{\lambda_2} L_{MODTRAN} RSR_{Aqua} d\lambda}{\int_{\lambda_1}^{\lambda_2} RSR_{Aqua} d\lambda}}}{n} \qquad n = number\ of\ atmospheric\ profiles \tag{4}$$

where $L_{MODTRAN}$ is the hyperspectral profile simulated using MODTRAN, λ_1 and λ_2 denote the wavelength range of the spectral channel, and RSR_{Terra} and RSR_{Aqua} define the RSR for the TEB that is being spectrally matched between the MODIS sensors. Once the SBAF is computed for all the MODIS TEBs, it can be used to correct either the Terra or Aqua MODIS radiances as follows:

$$L_{MODIS_{corr}} = L_{MODIS} \times SBAF \tag{5}$$

where L_{MODIS} is the Terra or Aqua MODIS radiance and $L_{MODIS_{corr}}$ is the spectrally corrected radiance to match its equivalent Terra or Aqua MODIS band. In the case of this study, the SBAF were derived as Terra-to-Aqua ratios, meaning that we apply the SBAF in Equation (5) to the Terra radiances to correct them. Afterward, the radiances can be converted to BT using Planck's law.

Numerous studies have shown that the MODIS Atmospheric Profile product correlates quite well with both radiosonde and Global Positioning System measurements over

Germany, Costa Rica, China, and the Iberian Peninsula, to name a few locations [35–38]. Moreover, it has been demonstrated that the MODIS Atmospheric Profile product provides similar results to those produced by satellite derived profiles from the Atmospheric InfraRed Sounder and five reanalysis profiles (the European Centre for Medium-Range Weather Forecasts (ECMWF), the Modern-Era Retrospective analysis for Research and Applications, Version 2 (MERRA2), the National Centers for Environmental Prediction (NCEP)/Global Forecasting System (GFS), NCEP/Final Operational Global Analysis (FNL), and NCEP/Department of Energy (DOE)) [39]. Hence, while using the ECMWF profile (or any other "external" source) makes logical sense because it does not come from MODIS, the analyses themselves will not change much, since the atmospheric transmittance, upwelling and downwelling radiances, and water vapor content are only slightly larger for MODIS when compared to ECMWF, and the impact caused by their differences on higher level products such as land surface temperature is smaller than 0.3 K.

3.3. Data Processing

The data used in this paper are the MODIS C7 L1B data. The L1B data are for an ocean scene, Dome C, and matching SNO with the IASI instrument. Since the NASA MODIS C7 L1B products are not officially available, the data used for this assessment were processed internally by the MCST using the officially delivered calibration LUT. The data cover both MODIS missions from 2003 to 2023. The measurements are monthly averaged, and the time series were generated for both instruments. This process applies to all three intercomparison references (i.e., ocean, Dome C, and IASI). All comparisons were made on a month-to-month basis. These data were used to generate all time series and allowed for direct MODIS-to-MODIS monthly comparisons, since the two instruments have different overpass times.

As mentioned previously, the IASI, onboard the MetOp satellite series, measurements were used as reference as well. The IASI data are Level 1C (L1C), and the matching SNO data with MODIS were downloaded from NOAA CLASS. The IASI L1C data spectrum and MODIS TEBs spectral response function are used to process the intercomparison between the IASI and MODIS TEB measurements. Since IASI data first became available after the currently operational MetOp-A satellite was launched back in 2007, all MODIS-to-IASI comparisons go from mid-2007 to the end of 2023.

4. Terra and Aqua TEBs: Trends and Intercomparison

4.1. Dome C

Figure 2 shows the trends in temperature difference between MODIS and coincident AWS measurements for Aqua and Terra bands 20, 25, 29, 30, 31, and 33 based on internally processed L1B using the C7 LUT. Each point represents a monthly average. These bands were selected to cover all the FPAs. Additionally, band 31 is included to demonstrate its stability, since it was used as a reference for all other bands. A noticeable seasonal oscillation can be seen, but the trends are stable over the mission. Bands 25, 30, and 33 are more sensitive to atmospheric conditions, and the magnitudes of the seasonal fluctuation are larger than other bands. A major improvement in C7 can be found for band 30 on both Aqua and Terra due to specific adjustments in the calibration coefficients (Table 2).

Figure 3 illustrates the trends of the relative difference between Terra and Aqua for MODIS bands 20, 25, 29 30, 31, and 33. Each point represents a monthly average after the double difference method is applied. The impact caused by spectral differences between the Terra and Aqua MODIS bands is corrected using the SBAF determined from MODTRAN simulations each month using the measured atmospheric profiles of temperature, elevation, pressure, water vapor mixing ratio provided by the MODIS atmospheric profile products.

The correction is applied by multiplying either Terra or Aqua MODIS observed radiance using the SBAF (as described in Section 3.2). The BT magnitudes of the SBAF correction are around 0.30 K for bands 24 and 25 over the Dome C site. For other TEBs, they are well within 0.10 K. Values of the relative difference between Aqua and Terra are well within 1.0 K (Table 4), indicating that their calibration is consistent at low temperatures. In addition, there is minimal impact because of atmospheric conditions over Dome C when compared with results over ocean, as discussed in Section 4.2.

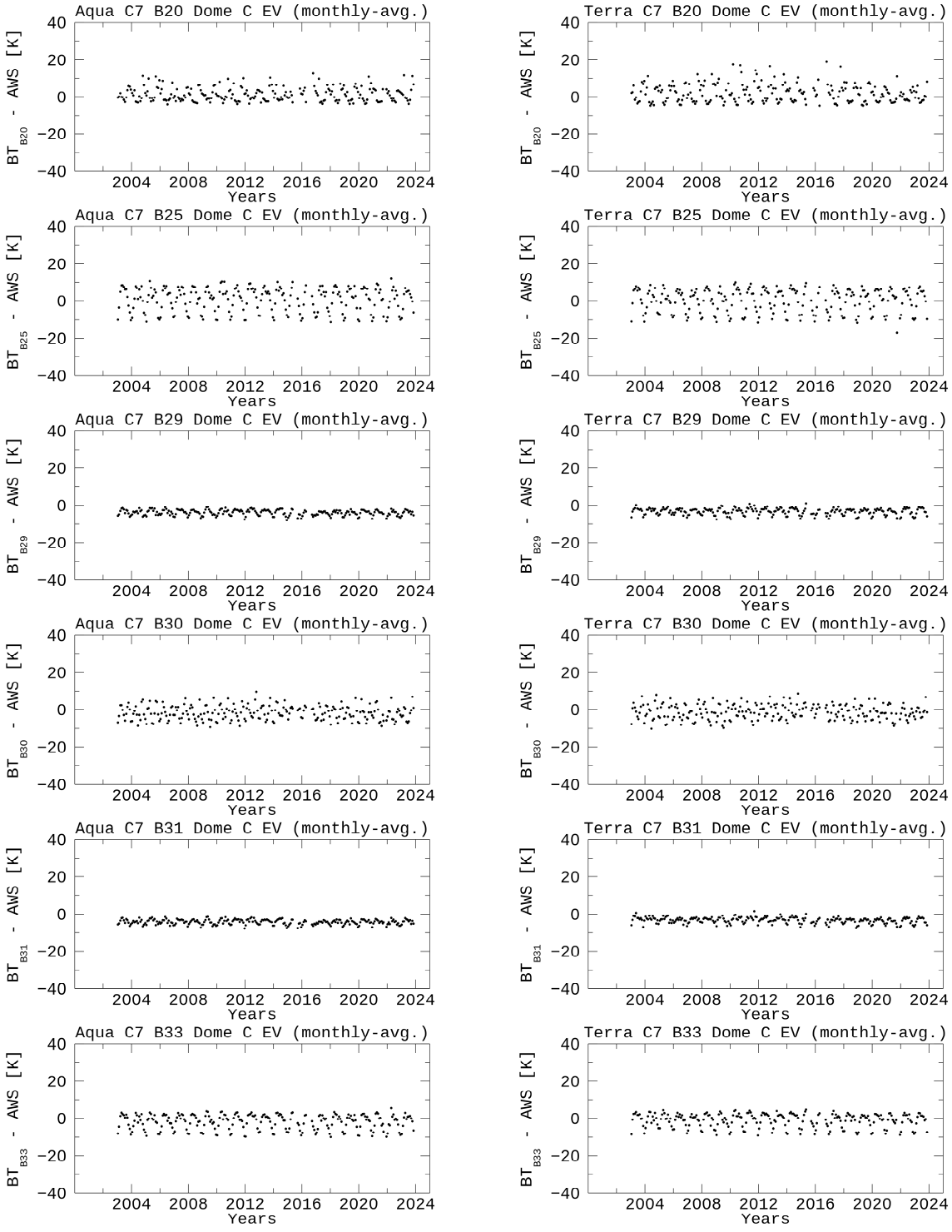

Figure 2. Aqua (**left**) and Terra (**right**) brightness temperature series over Dome C for MODIS C7 bands 20, 25, 29, 30, 31, and 33. All bands are referenced to AWS. Results are monthly averaged.

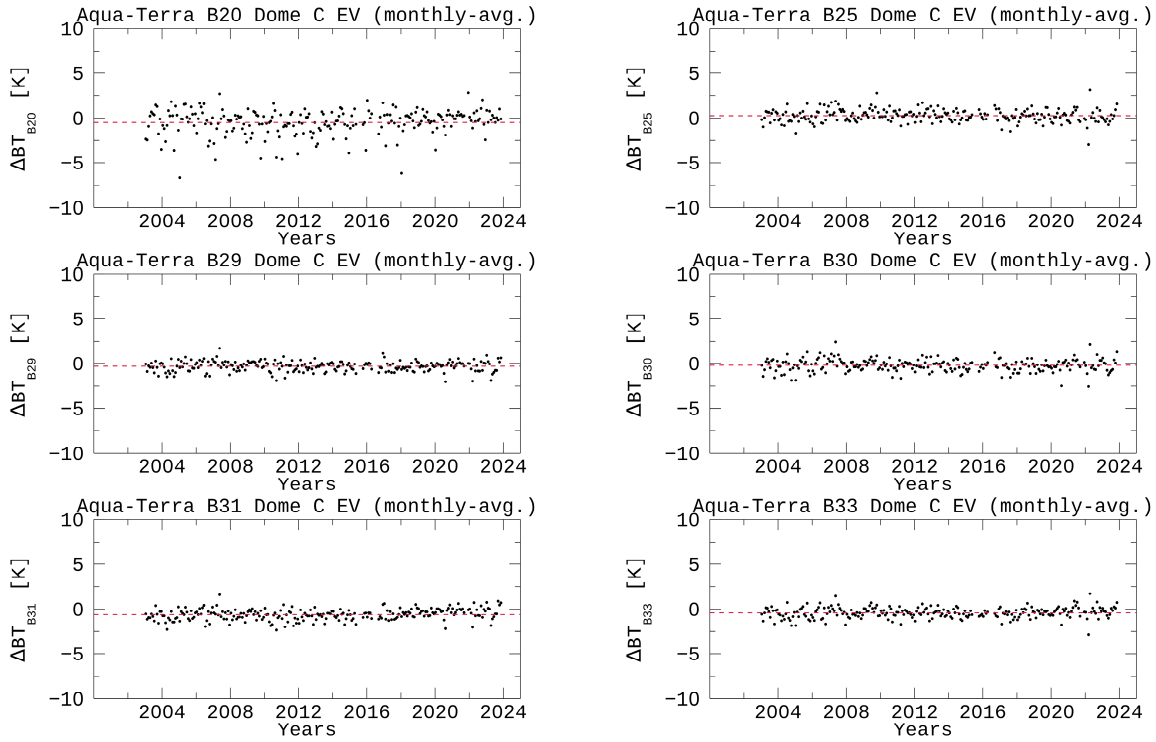

Figure 3. Aqua minus Terra brightness temperature series over Dome C for MODIS C7 bands 20, 25, 29, 30, 31, and 33. All bands are referenced to AWS. Red dashed horizontal line defines average Aqua minus Terra BT differences. Results are monthly averaged.

Table 4. Aqua minus Terra mission-long drifts and average Aqua minus Terra BT difference for all the MODIS C7 TEBs over Dome C. Drift values are calculated from linear fits to the mission-long data series. Avg. BT is the average of Aqua and SBAF adjusted Terra. Drift is the difference between the first and last year after the data have been fitted linearly. This applies to the A-T drift values as well. The Avg. BT diff is the red dashed line in the figures. Just the actual avg. BT difference.

Band	Avg. BT	Mission-Long Drift			Avg. BT Diff
		Aqua	*Terra*	*A-T*	
20	225.27	0.32	−1.14	1.46	−0.47
22	221.46	−0.46	−0.36	−0.10	0.71
23	221.52	−0.49	−0.24	−0.27	0.83
24	223.14	−0.88	−0.03	−0.85	0.01
25	222.42	−0.61	−0.22	−0.39	−0.28
27	224.81	−0.68	0.49	−1.17	0.85
28	222.07	−0.81	−0.19	−0.62	0.56
29	218.17	−0.76	−0.56	−0.20	0.31
30	220.66	−0.36	−0.04	−0.32	0.20
31	218.11	−0.47	−1.20	0.73	0.59
32	217.55	−0.41	−0.63	0.21	0.23
33	220.22	−0.50	−0.84	0.34	0.40
34	221.36	−0.42	−1.61	1.19	0.77
35	220.88	−0.73	−0.97	0.24	0.17
36	219.15	−1.34	−0.52	−0.82	0.25
All units in Kelvin					

4.2. Ocean

After the Terra and Aqua MODIS C7 series were generated over ocean for all TEBs, these were intercompared to assess the consistency between the two sensors. As mentioned previously, in order to mitigate known differences (i.e., overpass time, spectral) between the instruments, the intercomparison is performed at the monthly average level and the Terra radiances are adjusted using the SBAF to reduce spectral differences between the Aqua and Terra MODIS TEBs. Figure 4 illustrates the Aqua and Terra BT over ocean for sample bands 20, 25, 29, 30, 31, and 33. These bands were selected to cover all the FPAs. Additionally, band 31 is included to demonstrate its stability, since it was used as a reference for all other bands. In Figure 5, the Aqua minus Terra BT differences are shown for the same bands.

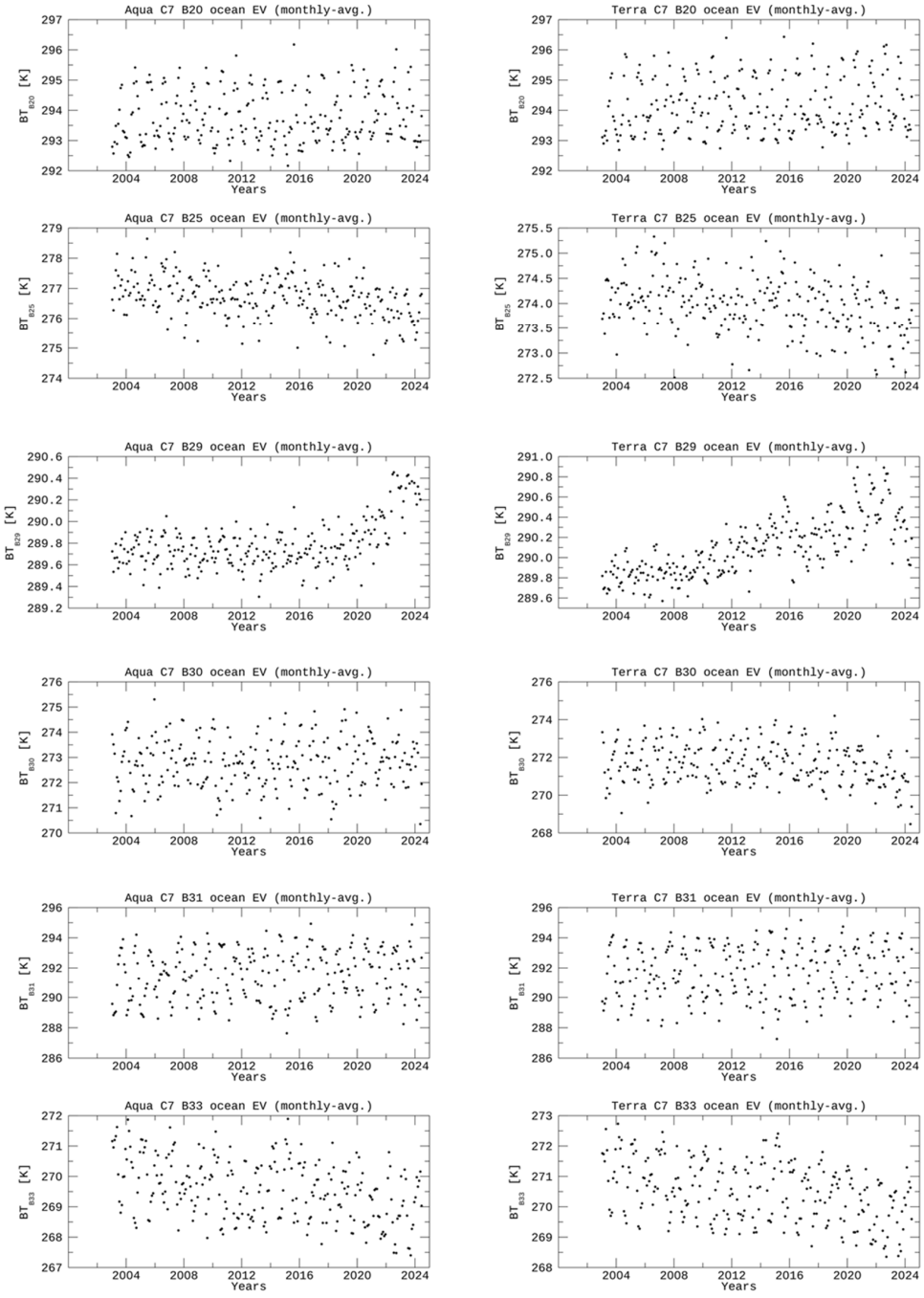

Figure 4. Aqua (**left**) and Terra (**right**) brightness temperature series over ocean for MODIS C7 bands 20, 25, 29, 30, 31, and 33. All bands are normalized (BT (band) = BT (band)—BT (band 31) + avg BT (band 31)) to band 31, except for band 31. Results are monthly averaged.

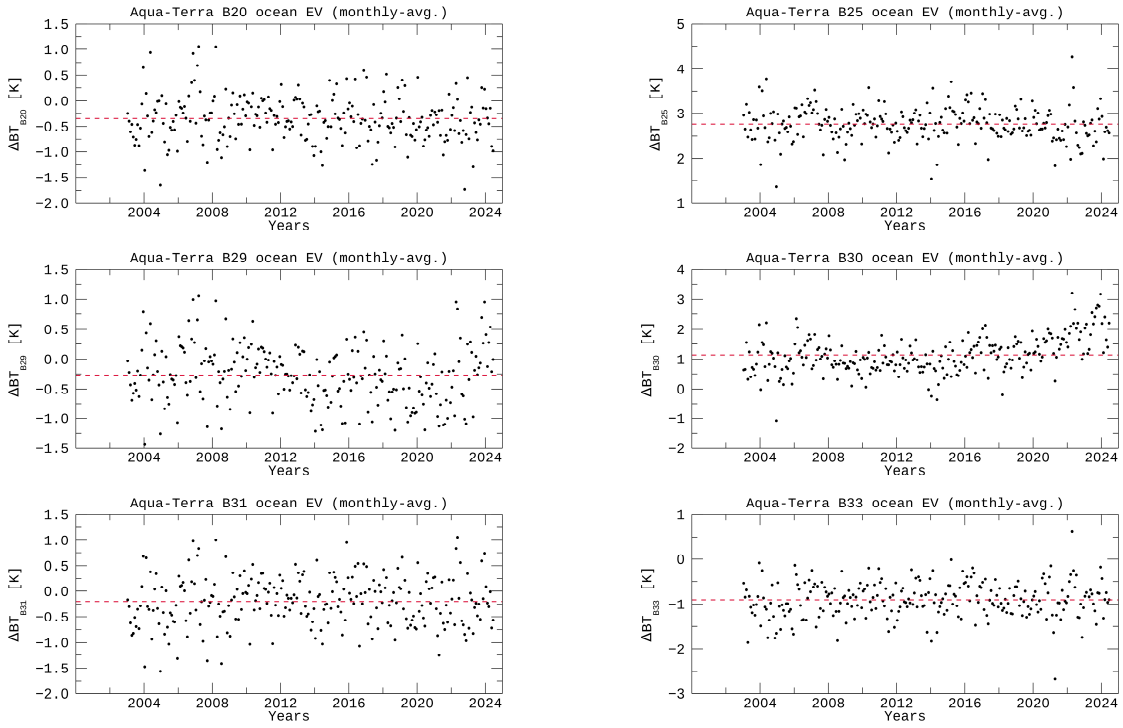

Figure 5. Aqua minus Terra brightness temperature series over ocean for MODIS C7 bands 20, 25, 29, 30, 31, and 33. All bands are normalized (BT (band) = BT (band)—BT (band 31) + avg BT (band 31)) to band 31, except for band 31. Red dashed horizontal line defines average Aqua minus Terra BT difference. Results are monthly averaged.

The intercomparison results in Figure 5 indicate that most bands are stable over the mission with little to no drift, except for band 29 (0.36 K and 0.75 K for Aqua and Terra MODIS, respectively) and all other water vapor affected bands (e.g., 24, 25, 27, 28, and the CO_2 bands), although this is more an artifact present over ocean rather than a calibration issue. Aqua MODIS band 30 also shows an upward trend more recently when compared to the same band for Terra MODIS; the timeline coincides with the Terra constellation exit maneuvers that saw the Terra MODIS PV bands performance improve. Table 5 summarizes the Aqua minus Terra mission-long drifts and average Aqua minus Terra BT difference for all the MODIS TEBs. Overall, all bands except for the PV LWIR bands show Aqua minus Terra drifts smaller than $\pm$0.33 K. Band 30 has the largest drift at 0.88 K, with bands 27 and 28 following with $\pm$0.64 K. When it comes to the average Aqua minus Terra BT differences, it has long been known that MODIS bands 24 and 25, as well as water vapor bands 27–28 and CO_2 bands 33–36 have spectral differences between Terra and Aqua that, despite being adjusted using the SBAF, continue to show differences as large as 2.75 K (band 25). Bands 24 and 25 have a slight RSR shift between MODIS instruments. Previous radiative transfer modeling of this bandpass shift has demonstrated that Terra will characteristically be 4 K and 2 K higher than Aqua for bands 24 and 25, respectively. Moreover, some other differences over ocean sites have been proven to be attributable to atmospheric temperature sensitivity [40,41]. All other bands show average A-T BT differences within approximately $\pm$0.5 K. It should also be noted that columnar water vapor plays a big role in these differences, particularly over the ocean.

Table 5. Aqua minus Terra mission-long drifts and average Aqua minus Terra BT difference for all the MODIS C7 TEB. Drift values are calculated from linear fits to the mission-long data series.

Band	Avg. BT	Mission-Long Drift			Avg. BT Diff
		Aqua	*Terra*	*A-T*	
20	293.99	0.11	0.40	−0.29	−0.38
21	293.48	0.65	0.45	0.20	−0.03
22	293.77	0.14	0.47	−0.33	−0.55
23	291.72	0.09	0.39	−0.31	−0.31
24	255.84	−1.42	−1.32	−0.10	2.06
25	275.32	−0.72	−0.51	−0.21	2.75
27	246.17	−0.71	−0.14	−0.57	−1.01
28	262.08	−0.88	−1.52	0.64	−0.10
29	289.94	0.36	0.75	−0.39	−0.31
30	272.23	0.25	−0.63	0.88	1.11
31	291.58	0.55	0.51	0.04	−0.20
32	290.99	−0.07	−0.12	0.06	−0.36
33	270.03	−1.19	−1.23	0.04	−0.94
34	258.78	−1.63	−1.66	0.04	−0.83
35	250.37	−1.65	−1.54	−0.11	−1.59
36	232.43	−1.45	−1.63	0.18	−1.06
All units in Kelvin					

4.3. IASI-MODIS

As mentioned in Section 3.1, the IASI instruments provide hyperspectral measurements in the IR spectrum that match with those retrieved by the MODIS TEB, and thus offer the distinct capability of assessing the MODIS TEB by comparing them to an external source—in this case, another sensor. As opposed to the assessment achieved by comparing different EV scenes as retrieved by MODIS, which has its own merits, an inter-sensor comparison provides additional insights. In this case, the MODIS and IASI SNO for each Aqua and Terra MODIS TEB (except for band 21) were directly compared (MODIS minus IASI), and afterwards the double difference method was used to cross-compare the MODIS instruments (Aqua minus Terra).

Figure 6 illustrates the Aqua-IASI and Terra-IASI BT difference time series for MODIS sample bands 20, 25, 29, 30, 31, and 33. The average BT for every SNO crossover between MODIS and IASI are shown. Just like in Section 4.2, these bands were selected to cover all the FPA, and band 31 is included to demonstrate its stability, since it is the MODIS band with the most stringent calibration requirements. Figure 7 displays the Aqua-IASI minus Terra-IASI BT difference time series for the same MODIS bands. Results indicate that all six bands shown are relatively stable throughout the mission with little to no drift, except for Aqua band 30 over recent years, which seems to be trending upward when compared to the same band for Terra MODIS, similar to the Aqua–Terra divergence discussed for the ocean trends for this band in Section 4.2. Furthermore, Figures 8 and 9 show the BT dependency over a broad BT range for these MODIS-IASI BT differences as a function of the MODIS BT for the same MODIS bands shown in Figures 6 and 7 for Terra and Aqua, respectively. Table 6 summarizes the average Aqua-IASI minus Terra-IASI BT difference as well as the BT dependency for these differences at different BT levels for all the MODIS C7 TEB. Overall, all bands except 23, 24, and 27 show average BT differences within ±0.5 K. Band 24 has

the largest average BT difference at 0.64 K. When it comes to the BT dependency, while all bands show more sensitivity at the lower temperature ranges, the results indicate no major issue across the broad BT range for all the MODIS TEBs in C7.

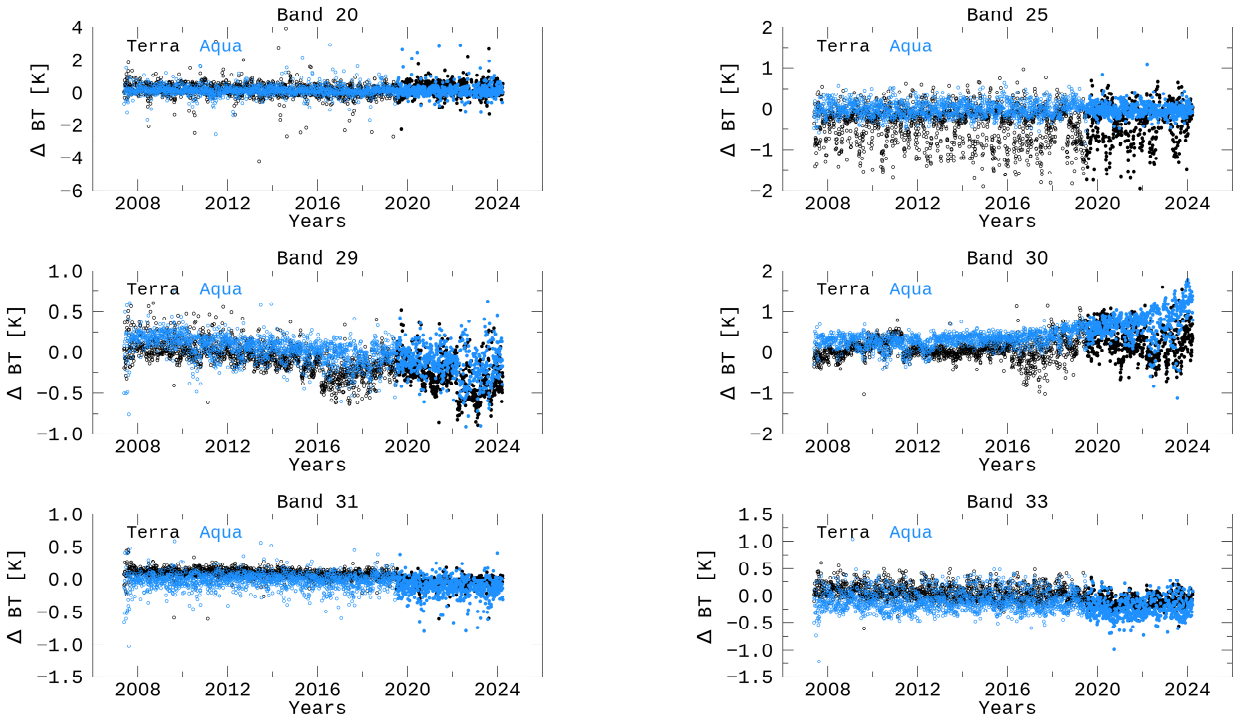

Figure 6. Aqua-IASI and Terra-IASI BT difference time series for MODIS sample bands 20, 25, 29, 30, 31, and 33. Average value for every SNO crossover between MODIS and IASI shown. Empty markers represent difference with IASI-A, while filled makers are used to denote IASI-C.

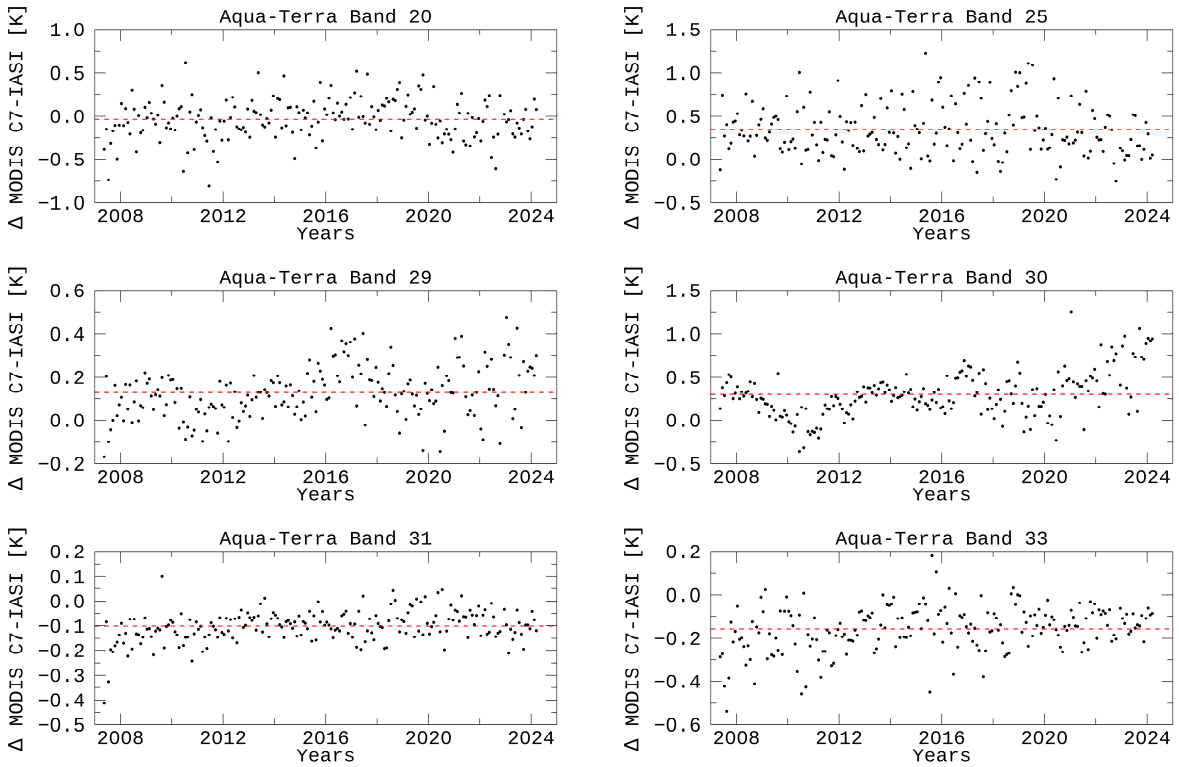

Figure 7. Aqua-IASI minus Terra-IASI BT difference for MODIS sample bands 20, 25, 29, 30, 31, and 33. Red dashed horizontal line defines average Aqua-IASI minus Terra-IASI BT difference. Results are monthly averaged.

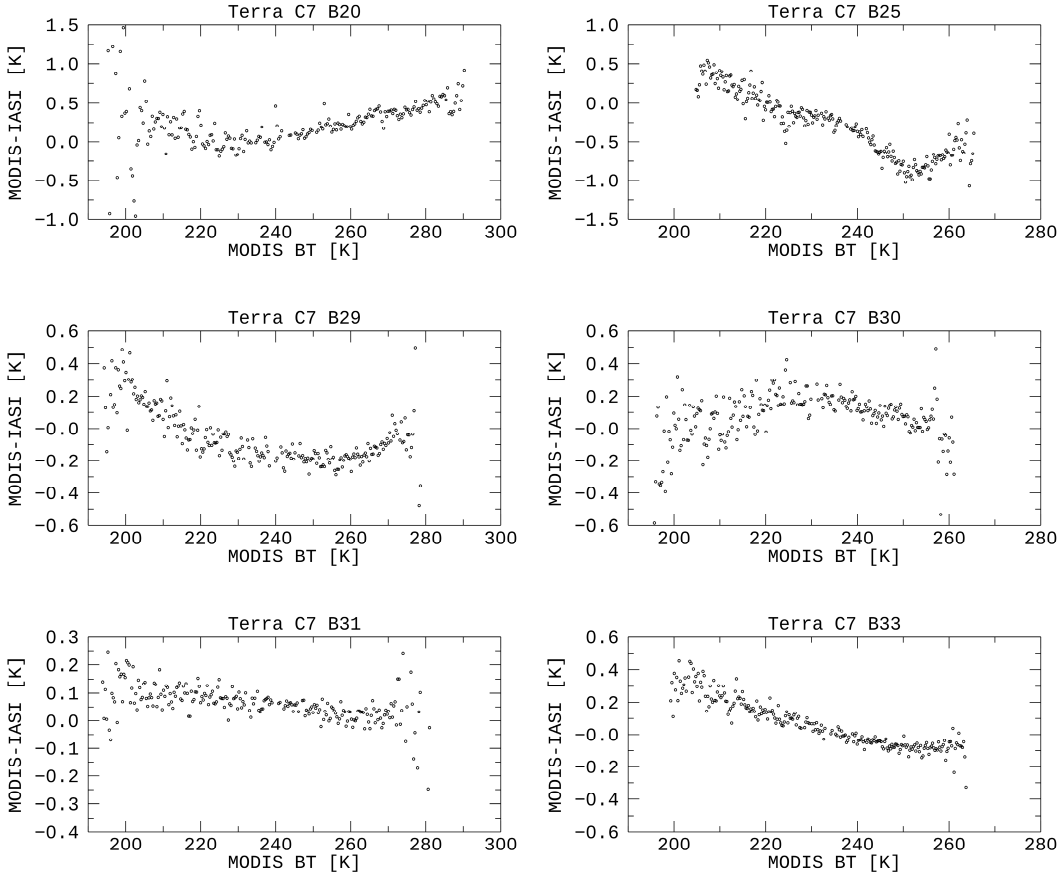

Figure 8. Terra-IASI BT difference as a function of Terra MODIS BT for MODIS sample bands 20, 25, 29, 30, 31, and 33.

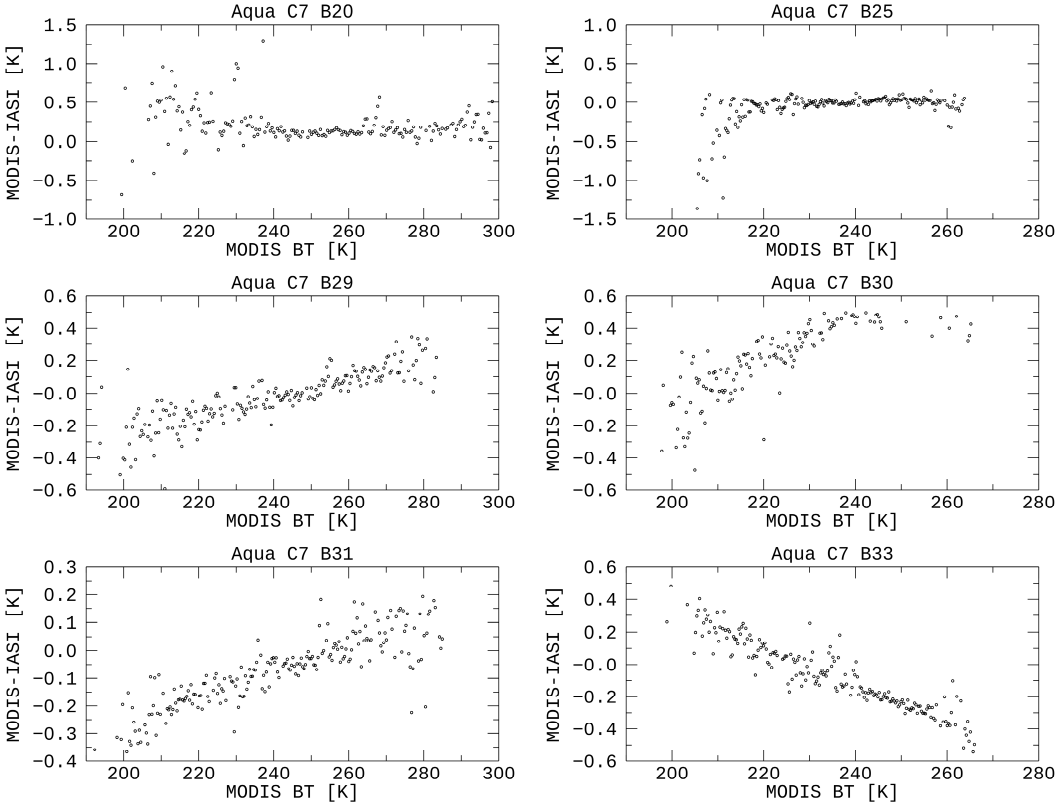

Figure 9. Aqua-IASI BT difference as a function of Aqua MODIS BT for MODIS sample bands 20, 25, 29, 30, 31, and 33.

Table 6. Aqua-IASI minus Terra-IASI BT difference as a function of BT for all the MODIS C7 TEBs.

Band	Avg. A-T BT Diff	Aqua-IASI Diff				Terra-IASI Diff			
		210 K	230 K	250 K	270 K	210 K	230 K	250 K	270 K
20	−0.04	0.46	0.27	0.10	0.18	0.23	−0.02	0.16	0.37
21	0.28	-	0.31	1.67	0.40	-	7.75	−0.20	0.18
22	0.39	0.99	0.36	0.12	0.07	0.31	−0.38	−0.18	−0.35
23	0.54	1.11	0.54	0.16	0.13	0.03	−0.38	−0.29	−0.43
24	0.64	−0.35	0.24	0.39	-	0.28	−0.38	−1.05	-
25	0.35	−0.17	0.00	0.03	-	0.29	−0.17	−0.80	-
27	−0.51	-	−0.34	0.94	-	0.34	0.17	-	-
28	−0.01	−0.18	−0.11	−0.04	-	0.20	0.02	−0.29	-
29	0.13	−0.19	−0.07	0.02	0.15	0.10	−0.12	−0.18	−0.09
30	0.30	0.05	0.34	0.44	-	0.03	0.18	0.07	-
31	−0.10	−0.22	−0.13	−0.02	0.07	0.10	0.07	0.04	0.03
32	−0.11	−0.09	−0.04	0.01	0.05	0.17	0.13	0.07	0.05
33	−0.16	0.20	−0.03	−0.24	−0.42	0.24	0.06	−0.08	-
34	−0.11	0.10	0.17	0.20	-	0.23	0.24	0.39	-
35	−0.14	0.14	0.28	0.65	-	0.14	0.39	0.73	-
36	−0.09	0.48	0.49	-	-	1.76	0.48	-	-
All units in Kelvin									

5. Discussion

The intersensor comparison indicates that only Aqua MODIS band 30 has drifted over recent years, while all other MODIS TEBs show excellent agreement with their IASI counterparts. The BT dependency analysis over a broad BT range demonstrated that, while the MODIS bands generally diverge from the IASI BT at the lower temperature ranges, there are no major issues across a comprehensive BT range for all the MODIS TEBs. Also noteworthy is the fact that MODIS band 31 displays excellent agreement with IASI, since this channel is not only largely used by the scientific community and is a surface band, but is widely used as a reference in many MODIS calibration studies and the published literature.

Results over warmer scenes (i.e., ocean) generally demonstrate reasonable stability amongst the Terra and Aqua MODIS TEBs. Aqua MODIS band 30 is the only exception, for it is drifting upward in recent years when compared to its Terra MODIS analog band. In the case of the Aqua MODIS PV LWIR bands, electronic crosstalk has increased dramatically since 2018, and especially after the March 2022 safe mode. Since the Terra and Aqua calibration algorithms are different, these discrepancies show up via the drifts, albeit not significant enough to warrant any action. Moreover, while there are some systematic biases between the Terra and Aqua MODIS bands that are affected by water vapor, this is not unexpected, since there are differences between the relative spectral response of the two sensors for these TEBs.

Trending results from the Dome C cold scenes show an expected noticeable seasonal oscillation, but the trends are stable over the mission. A major improvement in the band 30 stability in C7 (drifts of −0.36 K and −0.04 K for Aqua and Terra, respectively) over the previous C6.1 (−1.95 K and −2.40 K for Aqua and Terra, correspondingly) L1B is observed over the Dome C site for both Aqua and Terra due to specific adjustments to the calibration algorithm. Unlike the warmer scenes where the intercomparison results for a few water vapor sensitive bands are affected by atmospheric profiles, there is minimal impact due to

atmospheric conditions over Dome C, indicating one unique advantage of using the site to track sensor calibration stability and consistency.

6. Summary

The calibration consistency between satellite measurements from the two MODIS instruments is essential in generating accurate multi-year data records for long-term monitoring of the Earth's L1B data products. The Terra and Aqua MODIS TEBs are assessed and compared using measurements over Dome C and the ocean, as well as SNOs with IASI as a reference. Mission-long trending and intercomparison results are presented and discussed. Results indicate that both sensors share consistent calibration and Earth measurements within their design specifications. Due to electronic crosstalk contamination, the PV LWIR bands show slightly larger drifts across different Earth scenes for both sensors. This artifact also has an impact on the Terra-to-Aqua MODIS consistency. These drifts have become significant in recent years and are the main reason for the discrepancies between the Terra and Aqua MODIS PV LWIR bands (over 1 K difference for bands 27 and 30 over ocean and 0.85 K for band 27 over Dome C). Moreover, due to the spectral response differences between Terra and Aqua MODIS, bands 24 and 25 show sizable differences between the two instruments. This effect is highly dependent on scene and temperature (e.g., over ocean scenes, the Terra and Aqua differences for these two bands are around 1 K). This thorough assessment serves as the most recent and robust record containing a summary of the MODIS TEB calibration performance and the consistency between the two MODIS sensors over various Earth view retrievals.

Author Contributions: Conceptualization, X.X.; Methodology, T.C., C.P.D. and A.W.; Formal analysis, T.C.; Investigation, T.C., C.P.D., A.W. and H.L.; Data curation, C.P.D.; Writing—original draft, T.C., C.P.D., A.W. and H.L.; Writing—review & editing, X.X.; Supervision, X.X.; Project administration, X.X. All authors have read and agreed to the published version of the manuscript.

Funding: This research received no external funding.

Data Availability Statement: The data used in this study are openly available in https://ladsweb.modaps.eosdis.nasa.gov/ and https://www.aev.class.noaa.gov/. The original contributions presented in the study are included in the article, further inquiries can be directed to the corresponding author.

Acknowledgments: The authors would like to thank MCST members for working on the Terra and Aqua MODIS TEB calibration and L1B products. We also appreciate Kevin Twedt and Amit Angal for their internal review.

Conflicts of Interest: Authors Tiejun Chang, Carlos Perez Diaz, Aisheng Wu and Hanzhi Lin are employed by the company Science Systems and Applications, Inc. The remaining authors declare that the research was conducted in the absence of any commercial or financial relationships that could be construed as a potential conflict of interest.

References

1. Barnes, W.L.; Salomonson, V.V. MODIS: A global image spectroradiometer for the Earth Observing System. *Crit. Rev. Opt. Sci. Technol.* **1993**, *CR47*, 285–307.
2. Barnes, W.L.; Salomonson, V.V.; Guenther, B.; Xiong, X. Development, characterization, and performance of the EOS MODIS sensors. *SPIE* **2003**, *5151*, 337–345.
3. Barnes, W.L.; Xiong, X.; Salomonson, V.V. Status of Terra MODIS and Aqua MODIS. *J. Adv. Space Res.* **2003**, *32*, 2099–2106. [CrossRef]
4. Xiong, X.; Angal, A.; Chang, T.; Aldoretta, E.; Geng, X.; Link, D.; Sun, J.; Twedt, K.; Wu, A. Twenty years of Aqua MODIS on-orbit calibration, performance, and improvements. In Proceedings of the Volume PC12264, Sensors, Systems, and Next-Generation Satellites XXVI, SPIE Remote Sensing, 2022, Berlin, Germany, 28 October 2022. [CrossRef]

5. Salomonson, V.V.; Barnes, W.L.; Xiong, X.; Kempler, S.; Masuoka, E. An overview of the Earth Observing System MODIS instrument and associated data systems performance. In Proceedings of the IEEE International Geoscience and Remote Sensing Symposium, Toronto, ON, Canada, 24–28 June 2002; pp. 1174–1176.
6. Canadell, J.G.; Monteiro, P.M.S.; Costa, M.H.; da Cunha, L.C.; Cox, P.M.; Eliseev, A.V.; Henson, S.; Ishii, M.; Jaccard, S.; Koven, C.; et al. Global Carbon and other Biogeochemical Cycles and Feedbacks. In *Climate Change 2021: The Physical Science Basis. Contribution of Working Group I to the Sixth Assessment Report of the Intergovernmental Panel on Climate Change*; Cambridge University Press: Cambridge, UK; New York, NY, USA, 2021; pp. 673–816.
7. Xiong, X.; Aldoretta, E.; Angal, A.; Chang, T.; Geng, X.; Link, D.; Salomonson, V.; Twedt, K.; Wu, A. Terra MODIS: 20 years of on-orbit calibration and performance. *J. Appl. Remote Sens.* **2020**, *14*, 037501. [CrossRef]
8. Xiong, X.; Angal, A.; Chang, T.; Aldoretta, E.; Geng, X.; Link, D.; Sun, J.; Twedt, K.; Wu, A. Aqua MODIS: 20 years of on-orbit calibration and performance. *J. Appl. Remote Sens.* **2023**, *17*, 37501. [CrossRef]
9. Xiong, X.; Chiang, K.; Guenther, B.; Barnes, W.L. MODIS thermal emissive bands calibration algorithm and on-orbit performance. In *Optical Remote Sensing of the Atmosphere and Clouds III*; Third International Asia-Pacific Environmental Remote Sensing Remote Sensing of the Atmosphere, Ocean, Environment, and Space: Hangzhou, China, 2003; Volume 4891.
10. Xiong, X.; Salomonson, V.V.; Chiang, K.; Wu, A.; Guenther, B.W.; Barnes, W. On orbit characterization of RVS for MODIS thermal emissive bands. In *Passive Optical Remote Sensing of the Atmosphere and Clouds IV*; Fourth International Asia-Pacific Environmental Remote Sensing Symposium 2004: Remote Sensing of the Atmosphere, Ocean, Environment, and Space: Honolulu, HI, USA, 2004; Volume 5652, p. 210.
11. Xiong, X.; Wu, A.; Guenther, B.; Barnes, W.L. On-orbit Monitoring of MODIS Thermal Emissive Bands Response Versus Scan Angle. In Proceedings of the Sensors, Systems, and Next-Generation Satellites XI; SPIE Remote Sensing, Florence, Italy, 26 October 2007; Volume 6744.
12. Chiang, K.; Xiong, X. Pre-launch characterization of Aqua MODIS scan mirror response versus scan angle for thermal emissive bands. In Proceedings of the Earth Observing Systems XII; Optical Engineering + Applications, San Diego, CA, USA, 27 September 2007; Volume 6677.
13. Xiong, X.; Wenny, B.; Wu, A.; Barnes, W. MODIS Onboard Blackbody Function and Performance. *Geosci. Remote Sens. IEEE Trans.* **2010**, *47*, 4210–4222. [CrossRef]
14. Xiong, X.; Wu, A.; Chang, T.; Wilson, T.; Li, Y.; Chen, N.; Shrestha, A.; Diaz, P. On-orbit calibration and performance assessments of Terra and Aqua MODIS thermal emissive bands. *J. Appl. Remote Sens.* **2021**, *15*, 014520–1-19. [CrossRef]
15. Chang, T.; Shrestha, A.; Diaz, C.; Chen, N.; Wu, A.; Wilson, T.; Li, Y.; Xiong, X. MODIS thermal emissive bands calibration improvements for Collection 7. In Proceedings of the Sensors, Systems, and Next-Generation Satellites XXV; SPIE Remote Sensing, Online, 12 September 2021; Volume 11858. [CrossRef]
16. Angal, A.; Xiong, X.; Chang, T.; Twedt, K.; Geng, X.; Wu, A.; Aldoretta, E. Terra and Aqua MODIS collection 7 level 1B algorithm. *J. Appl. Remote Sens.* **2022**, *16*, 37502. [CrossRef]
17. Chang, T.; Shrestha, A.; Diaz, C.P.; Lin, H.; Wu, A.; Li, Y.; Chen, N.; Wilson, T. Proposed Calibration Improvements for the MODIS Thermal Emissive Bands in Collection 7 Level 1B Processing. MCST Memo. 2024. Available online: https://mcst.gsfc.nasa.gov/sites/default/files/file_attachments/M1163.2.pdf (accessed on 1 October 2024).
18. Wilson, T.; Wu, A.; Shrestha, A.; Geng, X.; Wang, Z.; Moeller, C.; Frey, R.; Xiong, X. Development and Implementation of an Electronic Crosstalk Correction for Bands 27–30 in Terra MODIS Collection 6. *Remote Sens.* **2017**, *9*, 569. [CrossRef]
19. MODIS Thermal Emissive Band Crosstalk Workshop. MsWG Meeting. August 2018. Available online: https://mcst.gsfc.nasa.gov/meetings/modis-thermal-emissive-band-crosstalk-workshop (accessed on 1 October 2018).
20. Moeller, C.; Hook, S.; Tobin, D.; Walden, V. Assessing MODIS LWIR band calibration accuracy. In Proceedings of the Earth Observing Systems XI; SPIE Optics + Photonics, San Diego, CA, USA, 7 September 2006; Volume 6296. [CrossRef]
21. Hook, S.J.; Vaughan, R.G.; Tonooka, H.; Schladow, S.G. Absolute radiometric in-flight validation of mid infrared and thermal infrared data from ASTER and MODIS on the Terra spacecraft using the lake tahoe CA/NV USA automated validation site. *IEEE Trans. Geosci. Remote Sens.* **2007**, *45*, 1798–1807. [CrossRef]
22. Wenny, B.; Xiong, X. Using a Cold Earth Surface Target to Characterize Long-term Stability of the MODIS Thermal Emissive Bands. *IEEE Geosci. Remote Sens. Let.* **2008**, *5*, 162–165. [CrossRef]
23. Xiong, X.; Wu, A.; Wenny, B.N. Using Dome C for moderate resolution imaging spectroradiometer calibration stability and consistency. *J. Appl. Remote Sens.* **2009**, *3*, 033520. [CrossRef]
24. Shrestha, A.; Wilson, T.; Wu, A.; Xiong, X. Evaluating calibration consistency of Terra and Aqua MODIS LWIR PV bands using Dome C. In Proceedings of the Algorithms and Technologies for Multispectral, Hyperspectral, and Ultraspectral Imagery XXIV; SPIE Defense + Security, Orlando, FL, USA, 8 May 2018; Volume 10644.
25. Wenny, B.N.; Xiong, X.; Dodd, J. MODIS thermal emissive band calibration stability derived from surface targets. In Proceedings of the Sensors, Systems, and Next-Generation Satellites XIII; SPIE Remote Sensing, 2009, Berlin, Germany, 22 September 2009; Volume 7474. [CrossRef]

26. Díaz, C.L.P.; Xiong, X.; Wu, A.; Chang, T. Terra and Aqua MODIS Thermal Emissive Bands Calibration and RVS Stability Assessments Using an In Situ Ocean Target. *IEEE Trans. Geosci. Remote Sens.* **2022**, *60*, 4201614. [CrossRef]
27. Tobin, D.C.; Revercomb, H.E.; Knuteson, R.O.; Best, F.A.; Smith, W.L.; Ciganovich, N.N.; Dedecker, R.G.; Dutcher, S.; Ellington, S.D.; Garcia, R.K.; et al. Radiometric and spectral validation of Atmospheric Infrared Sounder observations with theaircraft-based Scanning High-Resolution Interferometer Sounder. *J. Geophys. Res.* **2006**, *111*, D09S02. [CrossRef]
28. Moeller, C.; Menzel, W.P.; Quinn, G. Review of Terra MODIS thermal emissive band L1B radiometric performance. In Proceedings of the Earth Observing Systems XIX; SPIE Optical Engineering + Applications, San Diego, CA, USA, 26 September 2014; Volume 9218. [CrossRef]
29. Li, Y.; Wu, A.; Xiong, X. Assessment of MODIS collection 6.1 thermal emissive band calibration using hyperspectral IASI observations. In Proceedings of the Sensors, Systems, and Next-Generation Satellites XXIV; SPIE Remote Sensing, Online, 20 September 2020; Volume 11530, p. 1153019.
30. Bromwich David, H.; Stearns, C.R. *Antarctic Meteorology and Climatology: Studies Based on Automatic Weather Stations*; American Geophysical Union: Washington, DC, USA, 1993. [CrossRef]
31. Chang, T.; Xiong, X.; Angal, A. Terra and Aqua MODIS inter-comparison using LEO-GEO double difference method. In Proceedings of the Sensors, Systems, and Next-Generation Satellites XXII; SPIE Remote Sensing, 2018, Berlin, Germany, 25 September 2018; Volume 10785. [CrossRef]
32. Xiong, X.; Cao, C.; Chander, G. An Overview of Sensor Calibration Inter-comparison and Applications. *Front. Earth Sci. China* **2010**, *4*, 237–252. [CrossRef]
33. Berk, A.; Conforti, P.; Kennett, R.; Perkins, T.; Hawes, F.; van den Bosch, J. MODTRAN6: A major upgrade of the MODTRAN radiative transfer code. In Proceedings of the 2014 6th Workshop on Hyperspectral Image and Signal Processing: Evolution in Remote Sensing (WHISPERS), Lausanne, Switzerland, 24–27 June 2014.
34. Borbas, E.; Menzel, P. *MODIS Atmosphere L2 Atmosphere Profile Product*; NASA MODIS Adaptive Processing System, Goddard Space Flight Center: Greenbelt, MD, USA, 2015. Available online: https://ladsweb.modaps.eosdis.nasa.gov/missions-and-measurements/products/MOD07_L2 (accessed on 1 October 2024).
35. Li, Z.; Muller, J.-P.; Cross, P. Comparison of precipitable water vapor derived from radiosonde, GPS, and Moderate-Resolution Imaging Spectroradiometer measurements. *J. Geophys. Res.* **2003**, *108*, 4651. [CrossRef]
36. Campos-Arias, P.; Esquivel-Hernández, G.; ValverdeCalderón, J.F.; Rodríguez-Rosales, S.; Moya-Zamora, J.; Sánchez-Murillo, R.; Boll, J. GPS Precipitable Water Vapor Estimations over Costa Rica: A Comparison against Atmospheric Sounding and Moderate Resolution Imaging Spectrometer (MODIS). *Climate* **2019**, *7*, 63. [CrossRef]
37. Hailei, L.; Shihao, T.; Shenglan, Z.; Hu, J. Evaluation of MODIS water vapour products over China using radiosonde data. *Int. J. Remote Sens.* **2015**, *36*, 680–690. [CrossRef]
38. Sobrino, J.A.; Jiménez-Muñoz, J.C.; Mattar, C.; Sòria, G. Evaluation of Terra/MODIS atmospheric profiles product (MOD07) over the Iberian Peninsula: A comparison with radiosonde stations. *Int. J. Digit. Earth* **2014**, *8*, 771–783. [CrossRef]
39. Yang, J.; Duan, S.-B.; Zhang, X.; Wu, P.; Huang, C.; Leng, P.; Gao, M. Evaluation of Seven Atmospheric Profiles from Reanalysis and Satellite-Derived Products: Implication for Single-Channel Land Surface Temperature Retrieval. *Remote Sens.* **2020**, *12*, 791. [CrossRef]
40. Wenny, B.N.; Wu, A.; Madhavan, S.; Xiong, X. Evaluation of Terra and Aqua MODIS Thermal Emissive Band Response Versus Scan Angle. In Proceedings of the Earth Observing Systems XIX; SPIE Optical Engineering + Applications, San Diego, CA, USA, 2 October 2014; Volume 9218.
41. Seemann, S.W.; Li, J. Operational Retrieval of Atmospheric Temperature, Moisture, and Ozone from MODIS Infrared Radiances. *J. Appl. Meteor.* **2003**, *42*, 1072–1091. [CrossRef]